Experimental Investigation of the High Performance Steam Injector Operation

Shuichiro Miwa*, Yuto Takeya, Hiroto Endo and Michitsugu Mori

Graduate School of Engineering, Hokkaido University
North 13, West 8, Kita-ku, Sapporo, Hokkaido 060-8628 Japan
*Corresponding Address: smiwa@eng.hokudai.ac.jp

ABSTRACT

Steam injector (SI) is a simply designed passive jet pump which operates without external power source or mechanical machineries. The SI utilizes direct contact condensation between steam and water-jet as a driving mechanism for the operation and is capable of discharging subcooled water at higher pressure than the inlets. From the lessons learned from the accident in Fukushima Daiichi Nuclear Power Plant followed by the Great East Japan Earthquake, one of the practical methods to enhance the safety of nuclear power plants is to develop and install passive coolant injection systems that are operable even during the station black out condition. In the present study, operation characteristics of the water-jet-centered SI system were investigated from both experimental and analytical approaches. The SI body was manufactured with stainless steel at a maximum operable pressure rating of 1.5MPa. The water injection nozzle was designed with shaft-driving mechanism, to adjust the axial location of the water supply within the SI body. High pressure steam was supplied to the SI from the once-through boiler, which is capable of supplying saturated steam at the pressure of 0.6MPa. Pressure and temperature measurements were conducted at inlet and outlet of the steam injector system as well as at the overflow port to investigate the operation mechanism of the SI at high pressure condition. Finally, experimental results were compared with 1-D analytical model to understand the physical laws driving the SI, and applicability of the SI system as the passive coolant injection system of nuclear power plant was investigated.

KEYWORDS
Steam Injector
Jet Pump
Gas-Liquid Two-phase Flow
Direct Contact Condensation
Passive Core Injection System

1. INTRODUCTION

In order to regain the trust of nuclear power and utilize it as the primary energy sources, nuclear power plants need to be equipped with passive decay heat removal system. Currently equipped passive safety system, such as isolation condenser (IC), needs to be relied on active controls or human operation intervention to guarantee its operation, as was the case for the Unit 1 of Fukushima Daiichi. In addition, due to its large scale system composition, it is quite challenging to install IC into existing light water reactors as an additional safety system. Another passive safety system, the reactor core isolation cooling system (RCIC), which injects coolant by turbine-pump driven by the steam, is not operable with low pressure steam and could not prevent the severer accident at Fukushima Daiichi. Other conceptual safety system such as Gravity Driven Cooling System (GDCS), proposed by GE-Hitachi Nuclear Energy, passively injects coolant by the gravity head. However, it requires rapid depressurization of the reactor pressure vessel (RPV) until it is equated with the containment pressure to function properly.

In order for above mentioned safety systems to be passively operable during the severe accident, there still remain large uncertainties. On the other hand, the steam injector (SI), which is a simply designed passive jet pump, can be potentially applied as a more reliable and promising passive safety coolant injection system. Some of the possible applications are depicted in Figures 1 and 2, for both the passive coolant injection system for RPV and IC pool.

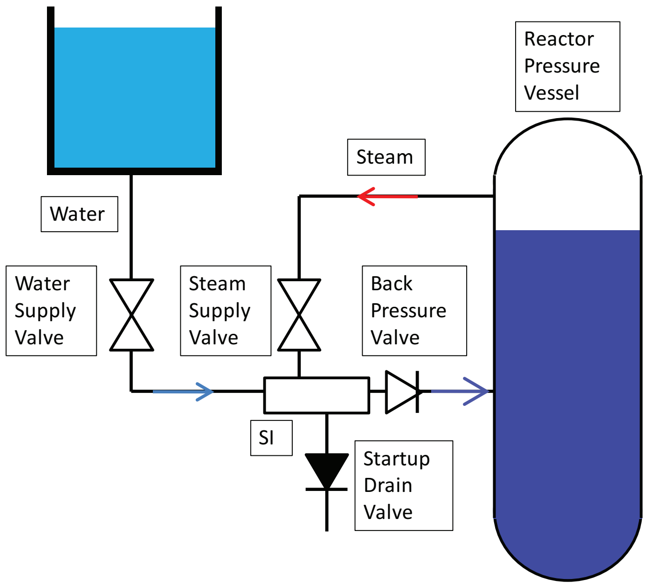

Figure 1: Conceptual diagram of SI-PCIS system (Narabayashi et al., 2000)

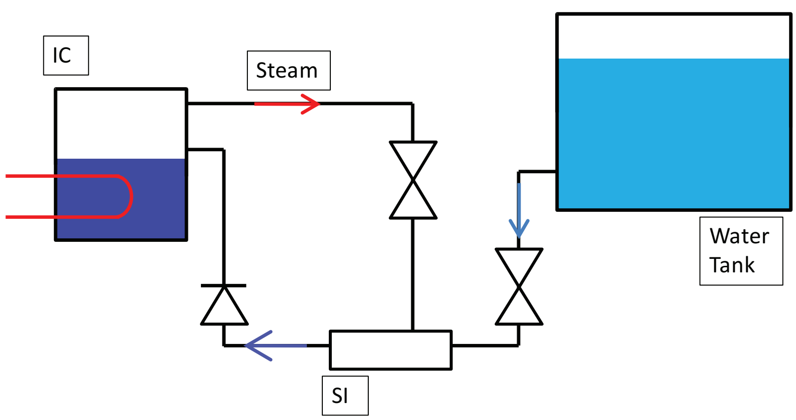

Figure 2: Conceptual diagram of SI system for IC (Narabayashi et al., 2000)

As was reviewed by Takeya et al. (2015), several types of SIs are proposed by various researchers up to now. Of all the SI propositions, water-jet centered SI equipped with overflow port shows rather stable start-up and operation of the SI. Figure 3 illustrates the schematic of water-jet centered SI unit. The unit composition can be subdivided into following four main sections. (a) Steam nozzle, composed of the annular zone created by the opening between water nozzle exterior and the SI inner wall for water-centered SI. Previous research confirms that the steam reaches nearly supersonic velocity and partially converting steam enthalpy into kinetic energy within the nozzle. (b) Water nozzle, where the water is injected, and forms high velocity water jet followed by a moderate acceleration through the nozzle. (c) Mixing nozzle, where the direct contact condensation process between steam and water takes place. This is where the interfacial mass, momentum and energy transfers take place due to the condensation, interfacial friction force, and heat transfer via temperature gradient. In an ideal SI operation, steam is completely condensed within this section and subsequently becomes single-phase subcooled liquid. Condensation location (or plane) is known as the "condensation shock" and proper control of its position is a key for the successful SI operation. (d) Diffuser, where the subcooled liquid pressure is further increased due to the diverging cross-sectional area. As can be seen, the fundamental concept of SI operation is through the direct contact condensation between compressible steam and incompressible water, and when it's operated, the unit is capable of pumping out the subcooled water at higher pressure than the inlet steam and water pressure. The operation can be sustained without any external electric or machinery power sources, which is the biggest advantage of the SI as a passive safety system compared to others.

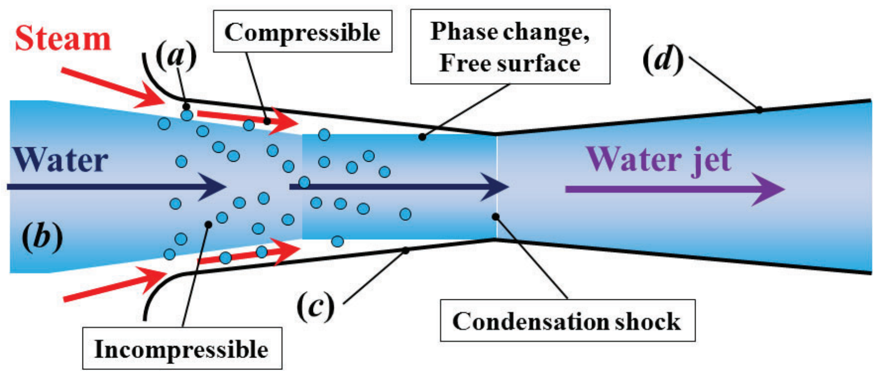

Figure 3: Schematic of the water-jet centered SI system, which is comprised of (a) steam nozzle, (b) water nozzle, (c) mixing nozzle, and (d) diffuser.

As can be reviewed from the available literature (Beithou et al., 2000; Cattadori et al., 1995; Deberne et al., 1999; Yan et al., 2005; Zhang et al., 2012), much advancement and improvement have been made for SI, such as converging-diverging angles, overflow port installation, and so on targeting various engineering applications. However, in order to utilize SI as a passive safety system of nuclear power plant, there still remain unknowns regarding its optimal design and operation conditions. One of the major reasons is the lack of experimental database at higher inlet steam pressure for the water-jet centered SI system. In order to optimize the SI operation, it is critical to collect fundamental dataset of various inlet conditions. For water-jet centered SI system operation, highest inlet steam pressure was reported by Abe et al. (2013) at 0.10 to 0.18 MPa range. In the present study, operation characteristics of the water-jet centered SI system were investigated in the steam pressure range of 0.18 to 0.53 MPa.

2. EXPERIMENTAL FACILITY AND INSTRUMENTATION

Figure 4 depicts the schematic diagram of the SI test facility. SI test section was manufactured by stainless steel with the maximum design pressure of 1.5MPa. Each component of the SI was designed with following dimensions; water nozzle exit diameter: 6.5mm, throat diameter: 6.0mm, mixing nozzle length: 180mm, and diffuser diameter: 14mm (Figure 5). Water nozzle was designed so that its position can be adjusted to change the steam nozzle cross section area (Figure 6). In the current test condition, water nozzle was pulled out for 30mm and the location was fixed throughout the experiment. Details of the design parameters are tabulated in Table 1. Inner surfaces of the SI were machine treated to eliminate rough surfaces. Overflow port was installed just upstream of the throat section. Importance of the overflow port was emphasized by many researchers, as it being a necessary component for the successful SI start-up.

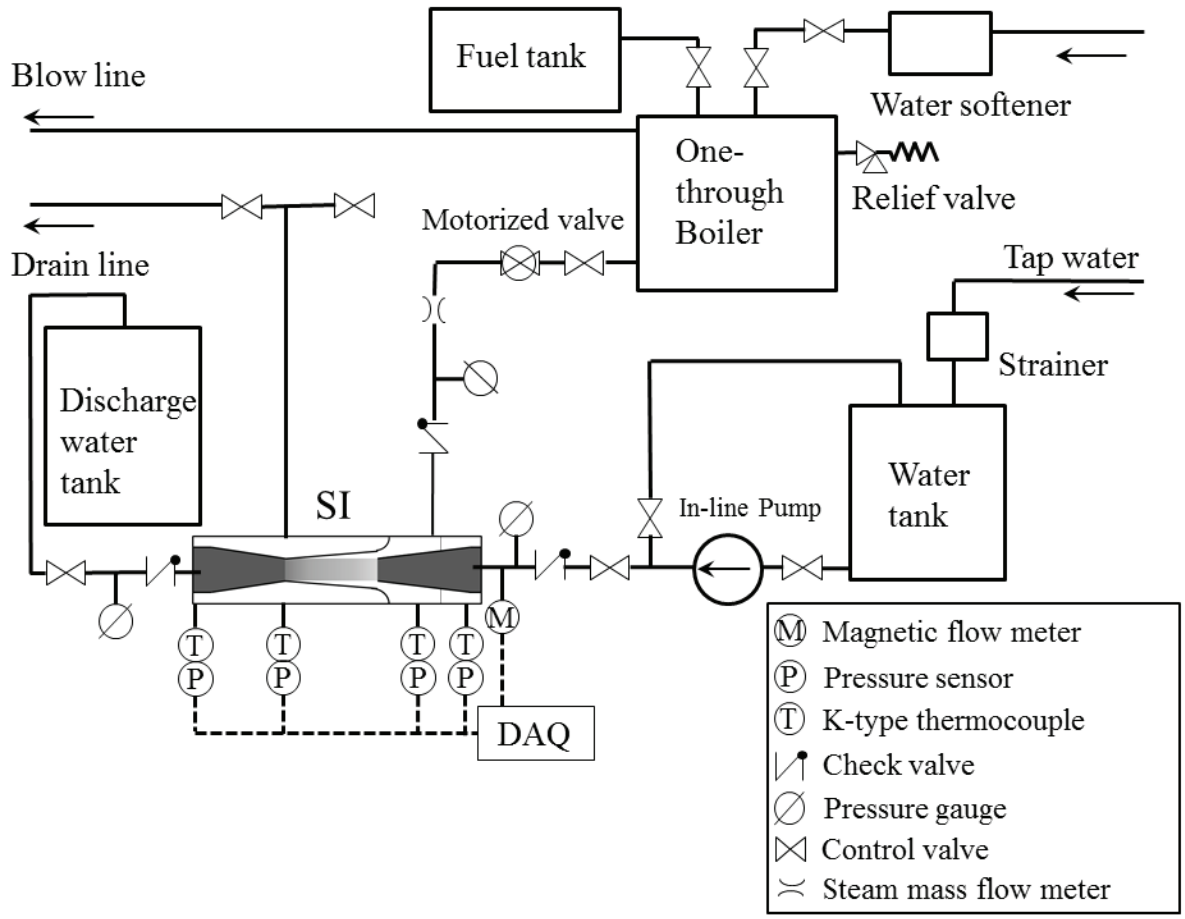

Figure 4: Schematic of the water-jet centered SI experimental facility

Steam is supplied from the one-through boiler (Miura, EH-F Series) which is capable of supplying the steam in the range of 0.49 to 0.88MP at maximum mass flow rate of 650kg/h. Steam flow was controlled by the motorized valve installed at the exit of boiler, and its mass flow rate was recorded by the steam mass flow meter (Azbil, STEAMcube) with the accuracy ±3% of reading. Water was supplied from the 1,000m^3 reservoir tank via inline pump (Tsurumi, TCR series) capable of pumping the water at maximum pressure of 1.5MPa. Volumetric water flow rate was recorded by the magnetic flow meter (Keyence, FD-M series) with the accuracy of ±1% of reading for the specified measurement range. At the SI test section, k-type thermocouples with the accuracy of 1ºC and digital pressure sensors (Keyence, GP-M series) with the accuracy of ±1% of reading were installed and connected to the data acquisition system for the measurement of local temperature and pressure at water nozzle inlet, steam nozzle inlet, overflow exit, and diffuser exit. Condensed fluid from the diffuser is subsequently discharged to the water tank, and its water level was monitored by the sight-glass. All the instrumentations were connected to the data acquisition board and simultaneous data recording was done for each test case.

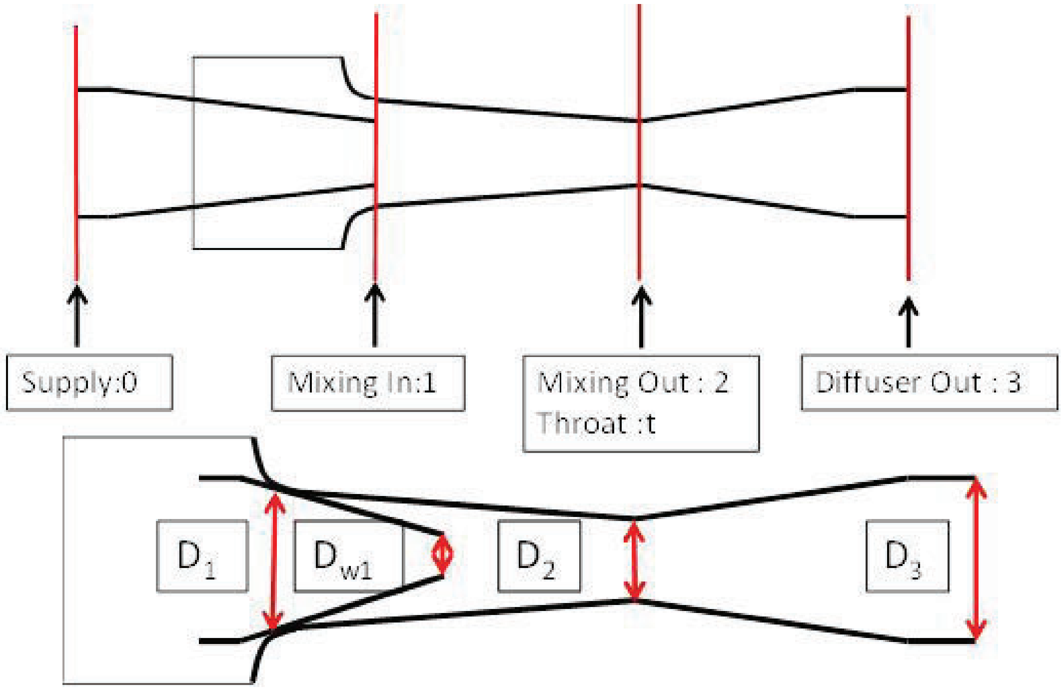

Figure 5: Schematic of the SI test section geometry

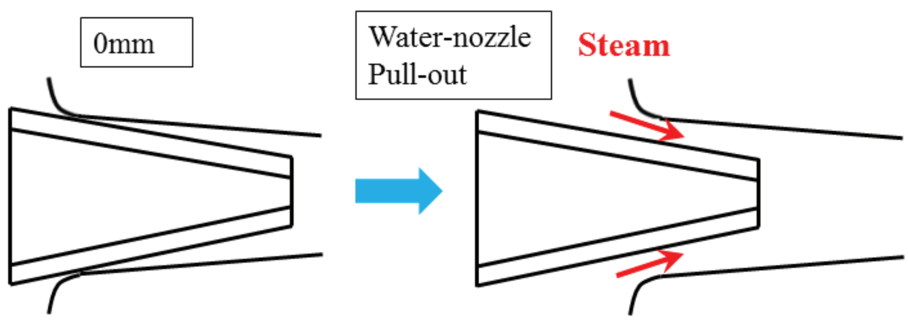

Figure 6: Water nozzle arrangement

Table 1: Design parameters of the SI test section

Water nozzle exit diameter (D_{w1})	6.5 mm
Mixing nozzle inlet diameter (D_1)	25.4 mm
Mixing nozzle exit diameter (D_2)	6.0 mm
Mixing nozzle throat diameter (D_t)	6.0 mm
Diffuser exit diameter (D_3)	14.0 mm

3. 1-D ANALYTICAL MODEL

In order to analyze SI's operational characteristics, analytical model proposed by Narabayashi et al. (1996) was applied to water-centered jet SI configuration, and 1-D code was developed. The scale information shown in Figure 5 and Table 1 is utilized for the geometrical input parameters. It is important to note that, current analytical model is applied for the SI analysis based on the following four major assumptions.

(1) Water pressure at the exit of water nozzle is considered to be at saturation state

(2) Steam is completely condensed within mixing nozzle and becomes single-phase. When the pressure is below the saturation pressure, fluid becomes two-phase flow.

(3) Steam pressure at the mixing nozzle inlet and average pressure within the mixing nozzle is equivalent to saturation pressure given by the throat temperature.

(4) Adiabatic condition is assumed at the wall boundaries of SI unit.

The model solves for mass, momentum and energy conservation equations for each component of the SI test section, as are described in this chapter.

Water Nozzle

Assume that water nozzle exit pressure to be at saturation state at the given water temperature. Then, water velocity can be calculated from Bernoulli's principle, and following expression can be obtained.

$$u_{w1} = \left[\frac{2v_{w0}(P_{w0} - P_{w1})}{1 + g_w} \right]^{1/2} \tag{1}$$

Then, mass flow rate of the water can be calculated as follows.

$$m_w = \frac{A_{w1} u_{w1}}{v_{w0}} = A_{w1} \left[\frac{2\left(P_{w0} - P_{w1}\right)}{v_{w0}\left(1 + g_w\right)} \right]^{\frac{1}{2}} \tag{2}$$

Steam Nozzle

When the steam pressure at steam nozzle exit is below the critical pressure, steam flow is at "choked" state. Based on previously reported work, in order to achieve stable SI operation, it is important to attain choked condition for steam inflow.

$$\frac{P_c}{P_{s0}} = \left[\frac{2}{(n+1)} \right]^{\frac{n}{(n-1)}}$$

$$P_{s1} < P_c \tag{3}$$

Then, mass flow rate of the steam at choked state can be given as follows.

$$m_s = 0.9 A_{snth} C_s P_{s0} \tag{4}$$

Here, *C*s is defined as,

$$C_s = \left[\frac{\frac{k(n-1)}{k-1}\left(\frac{2}{n+1}\right)^{\frac{n+1}{n-1}}}{RT_{s0}} \right]^{\frac{1}{2}} \tag{5}$$

and n is the polytropic index defined as follows.

$$n = \frac{k(1+g_s)}{1+kg_s} \tag{6}$$

g_s appearing in Eq. (6) represents the loss coefficient within the steam nozzle, which is calculated using the following expression.

$$g_s = 1 - \frac{h_{s0} - h_{s1}}{h_{s0} - h_{s1d}} = 1 - \frac{0.5\left(u_{s1}^2 - u_{s0}^2\right)}{h_{s0} - h_{s1d}} \tag{7}$$

Consequently, from Eq. (7), assuming that the steam velocity right at the steam nozzle (u_{s0}) is negligibly small, steam velocity at the steam nozzle exit can be approximated as follows.

$$u_{s1} = \sqrt{2(1-g_s)(h_{s0} - h_{s1d})} \tag{8}$$

Mixing Nozzle

Here, the region between plane 1 and 2 shown in the schematic of Figure 5 is considered as the mixing nozzle region. Then, mass, momentum, and energy equations can be written as follows.

[Mass conservation]

$$m_2 = m_s + m_w \tag{9}$$

[Momentum conservation]

$$\begin{aligned} &P_{s1}A_{s1} + P_{w1}A_{w1} + G_{s1}A_{s1}u_{s1} + G_{w1}A_{w1}u_{w1} \\ &= P_2A_2 + P_{12}\left(A_{s1} + A_{w1} - A_2\right) + G_2A_2u_2 + F_t \end{aligned} \tag{10}$$

Here, P_{12} represents the average pressure within the mixing nozzle section, and second term on the right hand side of the Eq. (10) represents the wall resistance force. Additionally, the last term appearing in Eq. (10) is the frictional loss term, which is defined as follows.

$$F_t = g_n A_2 \frac{u_2^2}{2v_2} \tag{11}$$

[Energy conservation]

$$m_s h_{s0} + m_w h_{w0} = m_2 \left(h_2 + \frac{u_2^2}{2} \right) \tag{12}$$

Assuming that the incoming fluids within the mixing nozzle becomes a single-phase subcooled fluid due to the direct contact condensation between steam and water, mixing nozzle exit temperature, T_2, can be estimated by neglecting the kinetic energy term, and using the specific heat value C_{p2} as follows.

$$T_2 = \frac{m_s h_{s0} + m_w h_{w0}}{m_2 C_{p2}} \tag{13}$$

In this analysis, complete condensation within the mixing nozzle was assumed for the SI operation, hence, if T_2 is higher than the saturation temperature at a given pressure of the mixing nozzle, calculation was terminated and SI is considered to be inoperative.

Diffuser

Since the fluid entering into the diffuser section is in subcooled state, Bernoulli's theorem can be utilized to calculate the exit pressure at the diffuser section. Third term appearing in the right hand side of Eq. (14) is the pressure loss at the throat and diffuser sections, respectively.

$$P_3 = P_2 + \frac{u_2^2}{2v_2} - \left(g_t + g_d \right) \frac{u_t^2}{2v_t} - \frac{u_3^2}{2v_3} \tag{14}$$

In order to conduct the analysis, SI design parameter tabulated in Table 1 as well as the actual operation condition values from the experiment was utilized for the analysis. In addition, loss-coefficient values utilized in the model were referred from Narabayashi et al.(1996) and JSME Mechanical Engineer’s Handbook (2006), that are tabulated in Table 2.

Table 2. Loss coefficient values used in SI analysis

Loss coefficient of steam nozzle (g_s)	0.37
Loss coefficient of water nozzle (g_w)	0.30
Loss coefficient of mixing nozzle (g_n)	0.05
Loss coefficient of throat section (g_t)	0.10
Loss coefficient of diffuser section (g_d)	0.14

4. RESULTS AND DISCUSSION

First part of the experiment was conducted to evaluate the operational characteristics of the SI and procedure is summarized as follows. As the SI system starts up, first, back pressure valve installed at the diffuser exit was set fully open and water was injected to the SI section through the water nozzle. During this stage, water smoothly flows through the SI section and flows out from both overflow port and diffuser section. Once the steady single-phase operation was confirmed, motorized valve installed at the steam line was opened to inject the steam into the SI section. As the steam flows through the mixing nozzle section, water flow from the overflow port is suddenly terminated and negative gauge pressure reading was confirmed at the port. Condensed subcooled water was ejected from the diffuser section. Once the steady-state condition is confirmed, back pressure valve installed at the exit of the diffuser section is slowly closed to add resistance and raise the exit pressure at SI. Exit pressure was continuously raised until the SI operation fails, and maximum discharged pressure was recorded.

Second, instead of continuously closing the back pressure valve, 40 seconds stabilization period was given at each valve opening setting. This was repeated until the SI operation gets terminated and overflow was observed. In the current study, maximum discharge pressure was defined as the pressure setting immediately before the overflow initiation. Mass flow rate of the water inlet was set to 0.4, 0.51, 0.62 kg/s, respectively and the temperature was maintained at 22ºC. Inlet steam pressure was chosen so that the steady and stable steam injection could maintain. Steam pressure in the range of 0.18 to 0.53 MPa with maximum standard deviation of 0.01MPa was supplied to the test section.

Figure 7(a) depicts the pressure conditions at "stable" operation of the SI system. As can be seen, exit pressure shown in magenta line is higher than the inlet steam (red) and water pressures (blue), which signifies that the SI is successfully operating as a passive pump. Gauge pressure at the overflow (green) is below zero, which implies that no flow is exiting from the port and all the incoming fluids are flowing out from the SI. It can be also confirmed from the temperature plot (Figure 7(b)) that steam is completely condensed within the SI unit, and fluid mixture is discharged at the temperature close to 50ºC.

Figure 8 depicts the pressure and temperature measurement right at the termination of the stable SI operation. This condition was achieved by slightly closing the back pressure valve after attaining the maximum discharge pressure. As can be seen, discharge pressure suddenly falls below the inlet fluids pressure and loses its functionality as a passive pump. At the same time, negative overflow pressure is no longer maintained and flow is discharged from the port. Large oscillation is observed at the water inlet pressure. This indicates that proper operation of the SI requires proper interfacial contact between steam and water to promote smooth interfacial mass, momentum and energy transfers. It can be also seen from the Figure 8(b) that even after the operation failure, SI's heat exchanging capability remains almost unchanged, where the fluid's exit temperature remains almost constant during the transient.

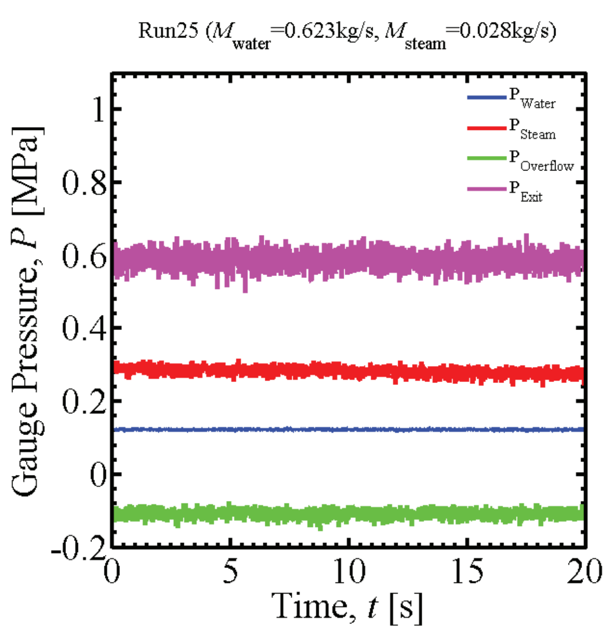

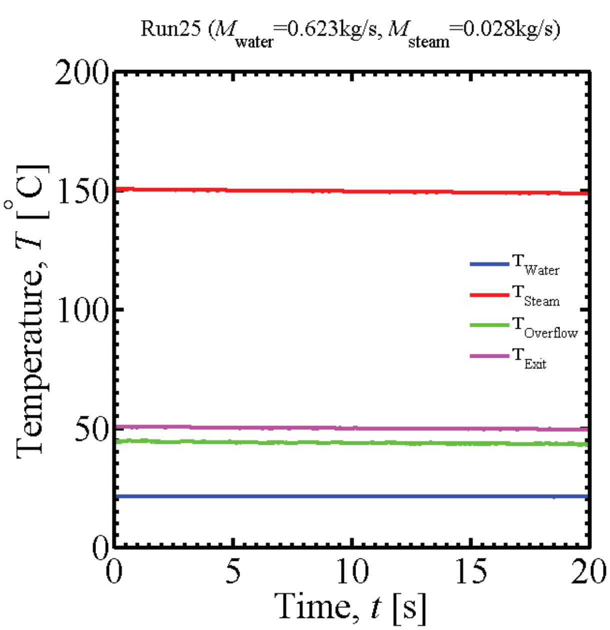

Figure 7: Plots of (a) Pressure and (b) Temperature at SI unit during the stable operation

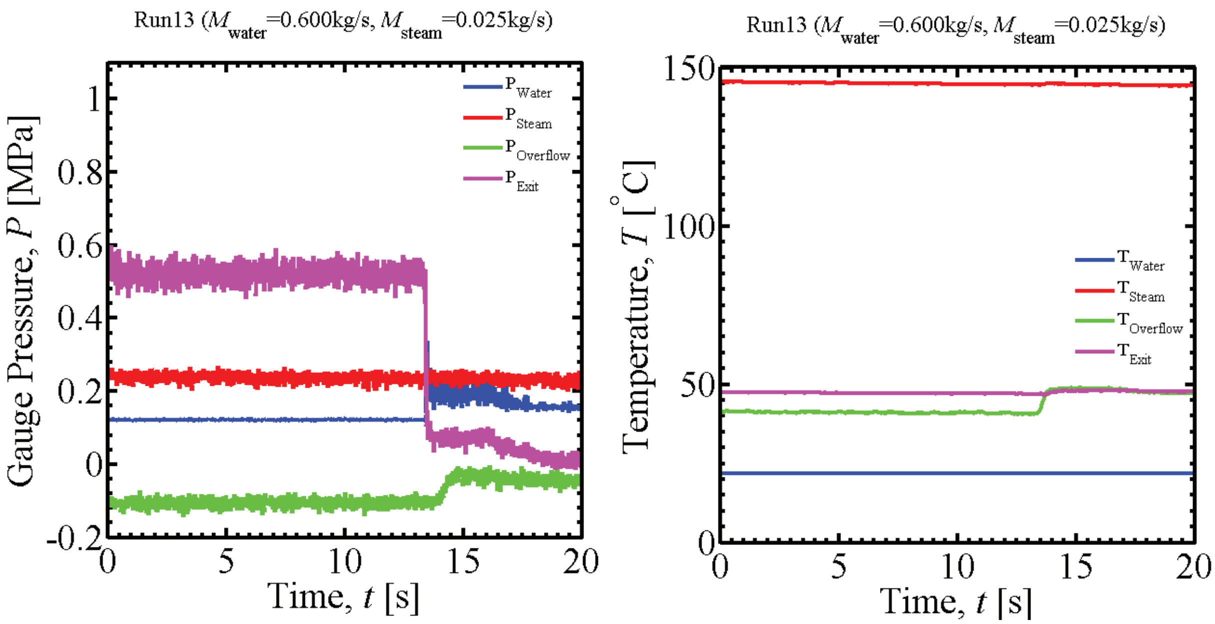

Figure 8: Plots of (a) Pressure and (b) Temperature at SI unit at the operation termination

Additionally, SI's capability as a "passive injection system" was assessed in the experiment by following procedure. Back pressure valve was partially closed prior to the SI start-up in order to achieve a passive pumping effect in the start-up. Following the water injection, motorized valve of the steam line was activated and the steam line was fully open. This operational methodology worked for some of the experimental conditions and confirmed the functionality of the SI system as a passive injection system. At some conditions, however, discharge pressure didn't surpass the inlet fluids pressure. Chaotic structure vibration was observed during the test, and it is encouraged to assemble the test facility with high natural frequency. Overall time history of the SI start-up to the termination is shown in Figure 9.

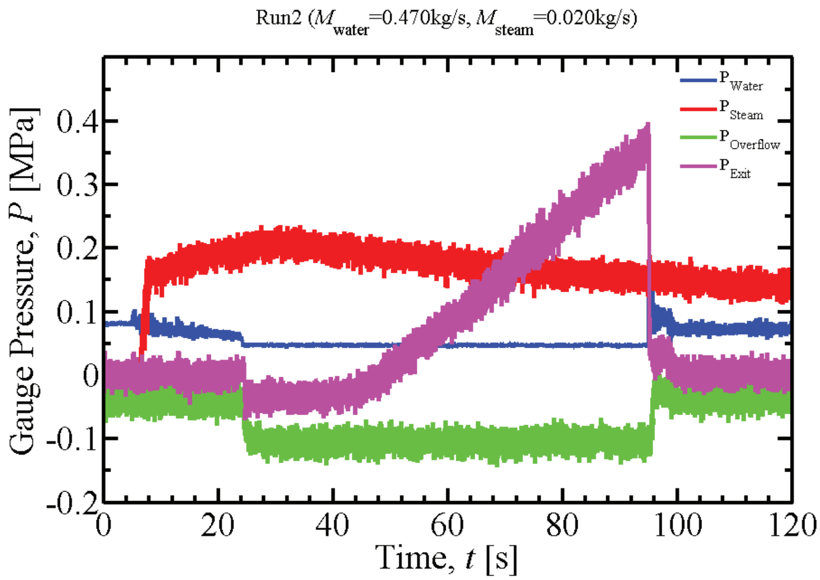

Figure 9: SI's pressure transient behavior from start-up to termination

Based on the experimental result, there exists critical back pressure condition at diffuser exit, in order for SI to maintain its stable operation as a passive pump. Hence, the model was utilized and compared with experimental data for assessing the dependency of inlet fluid condition towards the maximum SI pressure. Here, experimental condition at water mass flow rate of 0.4kg/s, 0.51kg/s, and 0.62kg/s at 22 ±1◦C. Inlet steam pressure was set in the range of 0.18~0.53MPa to cover the experimental condition. Figure 10 depicts the comparison between calculation and experimental results on maximum SI pressure at given inlet steam pressure. Clear dependency between maximum SI pressure and inlet steam pressure, as well as water mass flow rate, is shown from the figure, and they are linearly proportional to one another.

Pressure gain ratio of the SI system was obtained by taking the ratio between maximum SI pressure obtained from the experiment ($P_{E,MAX}$) and inlet steam pressure (P_S), which is defined as follows.

$$\Phi = \frac{P_{E,MAX}}{P_S} \tag{15}$$

The ratio basically describes the SI's pumping efficiency and the unit is operated as a pump (discharging higher pressure) when the value exceeds 1. As can be seen from Figure 11, lower inlet steam pressure leads to higher pressure gain ratio, and starts to diminish as the steam pressure increases. In the current experimental condition, Φ value was always greater than 1.4, and maximum value close to 2.5 was obtained. Hence, current design of the water-jet centered SI is capable of operating as a passive pump at given operation condition. Calculated maximum pressure and pressure gain ratio values showed good agreement with experimental data. However, the model presented in Narabayashi et al. [3] was originally developed for steam-jet centered SI, without overflow port. Hence, further improvement of the model is encouraged, but based on the current analysis, it was shown that the model can be utilized as an excellent tool to estimate discharge pressure of the water-jet centered SI system.

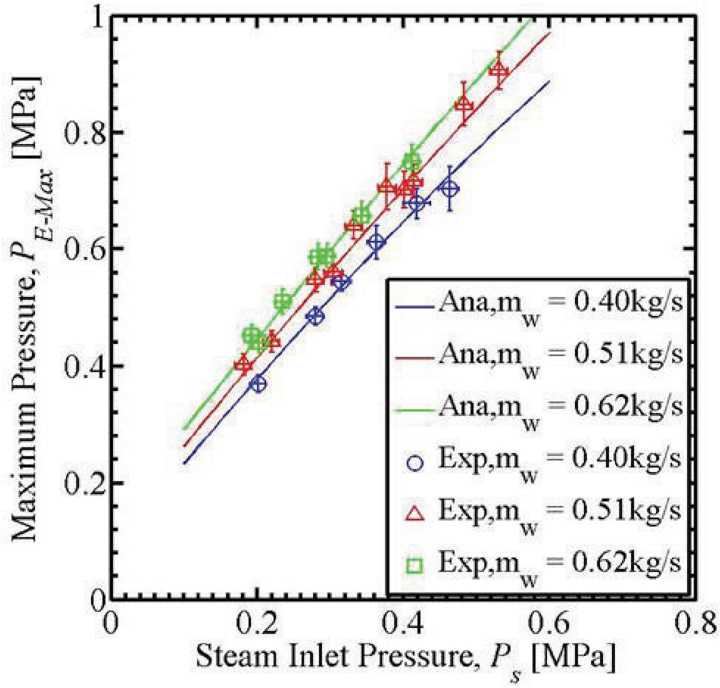

Figure 10: SI's maximum discharge pressure prediction based on inlet steam pressure.

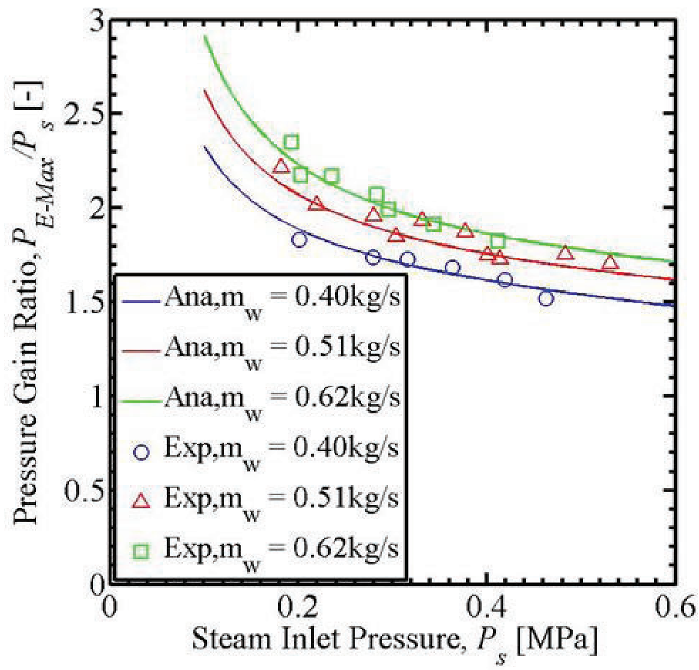

Figure 11: SI's pressure gain ratio prediction based on inlet steam pressure.

5. CONCLUSIONS

Steam injector can be operated as a passive jet pump without the use of AC power supply nor external machineries. In the current study, water-jet centered SI test section equipped with over flow port was manufactured and experiment was conducted at the maximum inlet steam pressure close to 0.6MPa, and discharge pressure close to 1.0MPa which hasn't been previously reported. Water-jet centered SI's high performance pumping and heat transfer capabilities were confirmed in the current work. Pressure gain ratio, as high as 2.5, was observed in the current experiment, and the incoming steam underwent complete condensation within the SI unit through direct contact condensation mechanism. Hence, current study shows SI's promising functionality as a new type of passive coolant injection system for advanced nuclear reactor safety. The model originally developed by Narabayashi et al. (1996) was adapted to the current SI configuration, and satisfactory calculation results predicting the maximum SI discharge pressure were obtained.

NOMENCLATURES

A_{snth} : Steam nozzle throat cross sectional area
A_{s1} : Steam nozzle exit cross sectional area
A_{w1} : Water nozzle exit cross sectional area
A_2 : Mixing nozzle throat cross sectional area
C_s : Correction factor for steam
Cp_2 : Specific heat of water at mixing nozzle throat
g_d : Loss coefficient of diffuser
g_n : Loss coefficient of mixing nozzle
g_s : Loss coefficient of steam nozzle
g_t : Loss coefficient of mixing nozzle throat
g_w : Loss coefficient of water nozzle
G_{s1} : Mass flux of steam
G_{w1} : Mass flux of water
G_2 : Mass flux at mixing nozzle throat
F_t : Friction factor
h_{s0} : Specific enthalpy of the inlet steam
h_{s1} : Specific enthalpy of steam nozzle exit
h_{s1d} : Steam specific enthalpy at steam nozzle exit
h_{w0} : Specific enthalpy of the inlet water
k : Specific heat ratio
n : Polytropic index
m_{of} : Mass flow rate at overflow
m_s : Mass flow rate at inlet steam
m_w : Mass flow rate at water nozzle exit
m_2 : Mass flow rate at mixing nozzle throat
m_3 : Mass flow rate past the overflow section
P_c : Critical steam pressure
P_{s0} : Supplying steam pressure

P_{s1} : Steam pressure at mixing nozzle inlet
P_t : Pressure at mixing nozzle throat
P_{w0} : Water pressure at water nozzle inlet
P_{w1} : Water pressure at water nozzle outlet
P_{12} : Average pressure within mixing nozzle section
P_2 : Fluid pressure near the mixing nozzle throat
P_3 : Discharge pressure of the SI
R : Gas constant for steam
T_{s0} : Supplying steam temperature
T_2 : Fluid temperature at mixing nozzle throat
u_{s0} : Steam velocity at steam nozzle inlet
u_{s1} : Steam velocity at steam nozzle outlet
u_t : Fluid velocity past the overflow section
u_{w1} : Water velocity at water nozzle exit
u_2 : Fluid velocity at mixing nozzle throat
u_3 : Fluid velocity at diffuser exit
v_t : Fluid specific volume at throat
v_{w0} : Fluid supplying water specific volume
v_2 : Specific volume at mixing nozzle throat
v_3 : Specific volume at diffuser

ACKNOWLEDGMENTS

Part of this research was performed by the Grants-in-Aid for Scientific Research of the Ministry of Education, Culture, Sports, Science and Technology of Japan.

REFERENCES

1. Y. Takeya, S. Miwa, T. Hibiki, and M. Mori, “Application of Steam Injector to Improved Safety of Light Water Reactors”, *Progress in Nuclear Energy*, **75**, pp.80-100 (2015)
2. T. Narabayashi, M. Mori, M. Nakamaru, S. Ohmori, “Study on two-phase flow dynamics in steam injectors II. High pressure tests using scale models”, Nuclear Engineering and Design, 200, pp. 261-271 (2000)
3. N. Beithou, H.S. Ayber, “A mathematical model for steam-driven jet pump”, *Int. J. Multiphase Flow*, **26**, pp.1609-1619 (2000)
4. J. Yan, S. Shao, J. Liu, Z. Zhang, “Experiment and analysis on performance of steam-driven jet injector for district-heating system”, *Appl. Therm. Eng*., **25**, pp.1153-1167 (2000)
5. Z. Zhang, D. Chong, J. Yan, “Modeling and experimental investigation on water-driven steam injector for waste heat recovery”, *Appl. Therm. Eng.*, **40**, pp.189-197 (2012)
6. Y. Abe, S. Shibayama, “Study on the Characteristics of the Supersonic Steam Injector”, *Nuclear Engineering and Design*, **268**, pp. 191-202 (2014)
7. T. Narabayashi, H. Nei, O. Ozaki, A. Shioiri, W. Mizumachi, “Study on High-Performance Steam Injector (1st Report, Development of Analytical Model for Characteristic Evaluation)”, *Trans. Jpn. Soc. Mech. Eng (in Japanese)*,**62**, pp.155-162 (1996)
8. The Japan Society of Mechanical Engineers, *JSME Mechanical Engineer’s Handbook,* Tokyo, Maruzen (2006)

9. G. Cattadori, L. Galbiati, L. Mazzocchi, P. Vanini, “A Single-Stage High Pressure Steam Injector for Next Generation Reactors: Test Results and Analysis”, *Int. J. Multiphase Flow*, **21**, pp. 591-606 (1995)
10. N. Deberne, J.F. Leone, A. Duque, A. Lallemand, “A model for calculation of steam injector performance”, *Int. J. Multiphase Flow*, **25**, pp.841-855 (1999)